

## Biosorption of Bromophenol Blue from Aqueous Solution using Flamboyant (*Delonix Regia*) Pod

### ABSTRACT

Matured flamboyant pods (FBP) activated with  $\text{ZnCl}_2$  were used for batch adsorption of Bromophenol blue (BPB) dye under the effects of concentration (10-200 ppm), contact time (20-300 min), biosorbent dosage (20-120 mg) and particle size (300-850  $\mu\text{m}$ ). The data obtained were fitted to Langmuir and Freundlich isotherm models as well as pseudo-first-order (PFO), pseudo-second-order (PSO), and Elovich kinetic models. The highest adsorption capacity and removal efficiency of 7.5762 mg/g and 75.76%, respectively, were obtained under the effects of initial dye concentrations. The correlation coefficient ( $R^2$ ) for the Langmuir and Freundlich isotherms are in the range 0.9938-0.9979 and 0.9895-0.9953, respectively, while,  $R^2$ , in the ranges 0.5931-0.815, 0.9962-1.000 and 0.8046-0.8828, were obtained for the PFO, PSO, and Elovich kinetic models, respectively. The order of fit of the kinetic models is PSO > Elovich > PFO. The study, thus suggests that flamboyant pod has a promising biomass for the remediation of dye-bearing industrial effluents.

**Keywords:** Biosorbent, Biosorption, Bromophenol Blue, *Delonix Regia*, Dye

### 1. INTRODUCTION

Anthropogenic activities have caused great harm to the quality of life in the terrestrial and aquatic environments [1]. Specifically, the generation of wastewater from various industrial activities has depleted the quality of freshwater resources considerably and dyes have been marked as important pollutants among the organic pollutants that are recalcitrant in the environment [2]. Dyes are coloured substances that have an affinity to the substrate to which they are applied. Dyes' colourations are due to their ability to appear to be coloured because they absorb some wavelengths of light more than other substances [3,4].

Many industries such as textile, leather, paper, printing, plastic, and so on generate a large amount of wastewater containing dyes. Dyes present water destined to be treated in municipal water treatment operations are difficult to treat due to their complicated chemical structures and, high visibility of these dyes, and undesirability [5]. Colour displayed by dyes in most water bodies makes such water unpleasant, while the level of concentration and exposure can manifest acute or chronic effects on exposed organisms [6, 7]. However, some of the dyes have been classified as being toxic and even carcinogenic [8, 9].

Some of the several techniques for the removal of dyes from wastewater include flotation, precipitation, oxidation, filtration, coagulation, ozonation, supported liquid membrane, and biological process. Meanwhile, biosorption process, which is a new and environmental-friendly method, has been deployed as the biosorption process is a promising process for the removal of dyes from effluent [10]. The biosorption process is an effective alternative method to replace the conventional methods, which are characterised by high cost and other more complicated operations compared to adsorption [11, 12]. Biosorption is the uptake or accumulation of chemicals by biomass. The process is similar to the adsorption process which involves uptake of toxic substances by biomass from contaminated fluid stream. It is cost-effective, easy to operate, simply designed, and insensitive to toxic substances.

Activated carbon is well known as the most widely used adsorbent and it has proven to be effective for the removal of dyes, due to its large surface area, microporous structure, and high adsorption capacity among others [13]. However, its high cost limits its usage in large-scale treatment process which is very limited due to its high cost of production and this has led to **the desire need** for alternative adsorbent materials that are cost-effective, efficient, and easily available for the production of the adsorbent materials for the

biosorption process [14]. Some of the proven efficiently adsorbent materials are peanut hull [15], orange and banana peels [16], pumpkin seed hull [17], and *Posidonia Oceanica* (L.) fibre [18].

Researchers have used several biosorbents to remove dyes from aqueous solutions for its good adsorption behavior and easy recovery of sorbent for further treatment. Surface characteristics of activated carbon make them versatile biosorbent in the treatment of pollutants such as dyes. The biosorption method has proved to be an excellent way of treating industrial waste effluents, offering significant advantages like low-cost, availability, profitability, easy operation, and efficiency. Several researchers had used agricultural wastes to sequester potentially toxic elements from wastewater [19].

Flamboyant is a perennial plant with fast growth up to 10-15 m height. Its branches spread like an umbrella, providing shade beneath the parent trees and as such, it has become one of the important and widely cultivated ornamental trees widely grown in the tropics and some other parts of the world [20]. Flamboyant is characterised with corymbs, 15-30 cm long, and bear five equal petals fragrant flowers [21]. The corymbs is matured, after fertilisation, to produce a 30-70 cm long, strap-shaped and flattened pod (30-70 cm long), which houses about 50 leguminous seeds. The initially leathery pods are leathery, initially but developed into reddish-brown or black and woody, when ripe [21]. The matured pod sheds after ripen through the year and this litter the vicinities of the parent trees. Small quantity Few uses of the woody pod is used include as solid fuel in some rural areas, while however the remaining huge tonnes of these materials are heaped and burnt or left to litter unattended to in many places thereby giving the host environment, with and untidy look [22].

This development gap has to challenges of solid waste disposal problems in left most of the developing nations such as Nigeria, where the population of the flamboyant tree is high with a great challenge of solid waste disposal problems. However, from the biotechnology view, This development has necessitated the need for the conversion of these wastes to useful and value-added products, such as adsorbent that possess the potential of amelioration other environmental challenges such as water pollution [21]. Flamboyant pods have been prepared and characterised as adsorbent activated carbon or biosorbent for the remediation of wastewater containing various organic and inorganic pollutants [20]. Specifically, Pandimadevi, et al., [23]; Mithun, et al., [24]; Adebisi, et al., [25]; Syed, et al., [26]; Owoyokun, et al., [27]; Alade, et al., [20]; Sugumaran, et al., [28]; and Jimoh, et al., [29] have deployed activated carbon or biosorbent derived from the flamboyant pod for the removal of dyes (methylene blue, aniline blue), heavy metals ( $\text{Hg}^{2+}$ ,  $\text{Co}^{2+}$ ,  $\text{Cu}^{2+}$ , and  $\text{Pb}^{2+}$ ) and organic pollutants (naphthalene) from synthetic wastewaters.

Bromophenol blue is an organic chemical compound formed from the addition of produced by slowly adding excess bromine and to a hot solution of phenolsulfonphthalein in glacial acetic acid. It is largely used as a pH indicator, an electrophoretic colour marker, and an industrial dye [12].

The chemical formula, molar mass, boiling and melting point of Bromophenol blue is  $\text{C}_{19}\text{H}_{16}\text{Br}_4\text{O}_5\text{S}$  (Figure 1) and has a molar mass of  $669.96 \text{ g mol}^{-1}$ . It has a boiling and melting point of  $279^\circ\text{C}$  ( $534^\circ\text{F}$ ) and  $273^\circ\text{C}$  ( $523^\circ\text{F}$ ), respectively, while its absorbance is exhibited at maximum wavelength of 206, 283 and 424 nm [30]. As an industrial dye and at neutral pH, Bromophenol blue absorbs red light most strongly and transmits blue light. Solutions of the dye, therefore, are blue. At low pH, the dye absorbs ultraviolet and blue light most strongly and appears yellow in solution. In solution at pH 3.6 (in the middle of the transition range of this pH indicator) obtained by dissolution in water without any pH adjustment, bromophenol blue has a characteristic green red color, where the dye's apparent colour shifts depending on the concentration and/or path length through which the solution is observed and t. This gives the dye its phenomenon is called dichromatic colour characteristics. Bromophenol blue is one of the dye the substances with the highest known value of Kreft's dichromaticity index and this indicates that changes in its colour hues depends on the changes in . This means it has the largest change in color hue when the thickness or concentration of the observed sample increases or decreases [30].

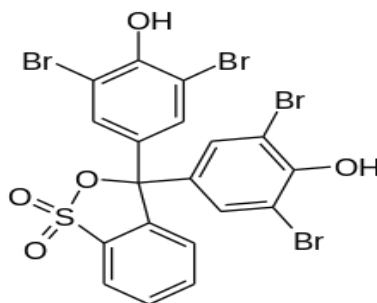


Figure 1: Structure of Bromophenol Blue Dye

Various studies on the removal of Bromophenol Blue dye from aqueous solution include the use of acid-activated clay, Gelidium Cartilagineum powder, Bentonite carbon composite material and UV-radiation with ZnO as a catalyst, have been reported by Okoye, et al., [31], Ch, et al., [32], El-Dars, et al., [33], and Mashkour, [34], respectively, but the efficacy of the flamboyant pod as biomass for the removal of Bromophenol blue has not been reported, thus this study was set up to demonstrate the effectiveness of these abundant materials for the removal Bromophenol blue from aqueous solutions.. In this study, the flamboyant pod was used as an alternative low-cost dye biosorbent for the **removal** of Bromophenol blue from aqueous solutions. The study was conducted in batch and necessary adsorption properties such as isotherms and kinetic models were investigated to evaluate the efficacy of the agricultural precursor in the treatment of aqueous solution containing dye such as Bromophenol blue dye.

## 2. MATERIAL AND METHODS

### 2.1 Material and Reagents

The basic material used for this study were matured Flamboyant pods (FBPs) that were found littering the vicinity of the parent trees in Mandate Area, Ilorin, Kwara State, Nigeria. Some of the reagents used are distilled water, zinc chloride ( $\text{ZnCl}_2$ ), bromophenol blue (BPB) tetraoxosulphate (VI) acid ( $\text{H}_2\text{SO}_4$ ), and Sodium hydroxide (NaOH). These reagents were of analytical grades and were used without further purification.

### 2.2 Experimental Methods

#### 2.2.1 Materials preparation

The raw FBPs were cut into pieces (3-4 cm), washed with tap water, and rinsed thoroughly with distilled water to remove any soluble materials attached to the FBP surface [35]. They were then dried to constant weight before being ground to smaller sizes in a mill and then sieved to obtain three different mesh particle sizes (850  $\mu\text{m}$ , 425  $\mu\text{m}$ , and 300  $\mu\text{m}$ ).

#### 2.2.2 Activation with Zinc Chloride

Zinc Chloride solution (0.1 M) was prepared by dissolving 13.63 g of  $\text{ZnCl}_2$  in 1 L distilled water. The dried flamboyant particle mixed with zinc chloride solution in a ratio of 3:50 (w/v). The mixture was kept at room temperature for 24 h and later boiled off in the Fume cupboard until it formed paste [20]. The mixture was allowed to cool and then washed with distilled water to remove excess reagent until the pH was stable between 6.9 and 7.1. The mixture was filtered and the residue, which is now the Activated Flamboyant Pod (AFBP), was then spread on an aluminium foil paper, and oven-dried at 105°C to constant weight and kept for further use [20].

## 2.3 Characterization

### 2.3.1 Moisture content determination

The FBP sample (0.1 g) was placed in a pre-weighed sample container and then charged into an oven at 105°C for 24 h [36, 37]. The sample was then removed and cooled in a desiccator, before being re-weighed. The amount of moisture removed was evaluated using Eq. (1) [38].

$$\text{Moisture content} = \frac{m_i - m_f}{m_i} \times 100\% \quad (1)$$

where,  $m_i$  = Mass of the initial sample and  $m_f$  = Mass of the final sample after drying

### 2.3.2 Determination of ash content

The FBP sample (2.5 g) was put in a pre-weighed porcelain crucible and then charged into a muffle furnace at 760°C for 90 mins **1.5 h**, for the samples to turn to ashes [39]. The crucibles were collected, after the required heating, and cooled in a desiccator and then weighed. The amount of ash was deduced according to Eq. (2).

$$\% \text{ Ash} = \left[ \frac{\text{Weight of sample remaining}}{\text{Weight of original sample}} \right] \times 100\% \quad (2)$$

### 2.3.3 Determination of volatile matter

The volatile matter was determined by taking 1.5 g of the FBP sample in a silica crucible with a porous silica cover and then heated for 7 min at a constant temperature of 925°C in a furnace. The crucible was collected and cooled in a desiccator then re-weighed [40]. The amount of volatile matter present in the sample was given as the difference in the masses of the crucibles before and after heating [23].

### 2.3.4 Determination of fixed carbon

The fixed carbon (F.C) represents the carbon content in a sample that has not combined with any other element (in a free state). The amount of fixed carbon in the FBP sample was computed by deducting the sum of the percentage of ash, moisture, and volatile matter content of FBP from a hundred percent as expressed in Eq. (3) [41].

$$\text{Fixed carbon} = 100 - (\text{moisture \%} + \text{ash \%} + \text{volatile matter \%}) \quad (3)$$

### 2.3.5 Surface Characteristic

Fourier Transform Infrared Spectroscopy (FTIR) was employed to study the surface chemistry of both raw and activated FBP samples [42, 43]. This will identify the main chemistry could be responsible for the adsorption process. The spectrum of the biosorbent was within the range of 400-4000 **cm<sup>-1</sup>** wave number. The comparison of the FTIR spectra of the FBPr<sub>aw</sub> (untreated) and AFBP activated with zinc chloride (treated) was done.

## 2.4 Preparation of Stock Solution of Bromophenol Blue (BPB) Dye

BPB dye stock solution was prepared by dissolving 1.0 g of BPB dye powder in 1.0 L of distilled water. Different concentrations such as 5, 10, 15, 20, 25, and 30 mg/L of the solution were prepared via appropriate dilution [44]. The absorbance of each dye concentration was recorded at 590 nm using UV/Vis spectrophotometer and the values obtained were used to develop the absorbance-concentration profile as the calibration curve used in this study [45].

## 2.5 Batch Adsorption Studies

Batch adsorption experiments for the removal of BPB using the activated FBP biosorbent were performed at selected contact time (10-270 min), initial concentration (5-30 mg/L), biosorbent dosage (100-700 mg) and particle sizes (300-850 µm) of the biosorbent. The required amount of the AFBP was added to 100 ml of different concentrations of BPB solutions and then agitated at pre-set speed (rpm). The dye solution was then decanted and centrifuged at 1,500 rpm for 30 min and the absorbance of the supernatant was then analysed using a UV-Vis spectrophotometer at 590 nm [46]. The unabsorbed amount of the BPB was quantified accordingly. Adsorption capacity and percentage removal were then determined accordingly Eq. (4-5) [31].

$$q_e = (V(C_o - C_e)) / W \quad (4)$$

$$\text{Removal (\%)} = [(C_o - C_e) / (C_o)] \quad (5)$$

where, V is the volume (L) of dye solution used; C<sub>o</sub> and C<sub>e</sub> are initial and final concentrations of the BPB dye in solution (mg/L), W is the amount (g) of AFBP used [33].

### 2.5.1 Effect of initial dye concentration

The effect of initial dye concentration (5-30 mg/L) on adsorption of BPB was studied by mixing 300 mg of FBP in a 250 ml flask containing 100 ml of the desired dye solution at room temperature and agitated at 200 rpm for 1 h [34, 47]. The dye solution was then decanted and centrifuged at 1,500 rpm for 30 min and the absorbance of the supernatant was then analysed using a UV-Vis spectrophotometer at 590 nm [46]. The unabsorbed amount of the BPB was quantified accordingly

### 2.5.2 Effect of contact time

The effect of contact time (10-270 min) was studied by mixing 100 ml of the BPB solution with 300 mg of the AFBP in different 250 ml conical flask [48]. Each flask was withdrawn from the shaker, at a pre-set time and the dye solution was decanted, centrifuged at 1,500 rpm for 30 min and the absorbance of the supernatant was analysed using UV-Vis spectrophotometer at 590 nm [46].

### 2.5.3 Effect of biosorbent dosage

The effect of AFBP dosage on the removal of BPB from the aqueous solution was studied by adding different dosages (100 to 700 mg) of the AFBP to 100 ml of 20 mg/L BPB dye solution in 250 ml flask at room temperature. The mixture was agitated on the rotary shaker at 200 rpm for 1 h. The dye solution was then decanted and centrifuged at 1,500 rpm for 30 min and the absorbance of the supernatant was analysed using a UV-Vis spectrophotometer at 590 nm [46].

### 2.5.4 Effect of particle size

Each adsorption experiment was conducted using 850 µm, 425 µm, and 300 µm particle size of the AFBP to evaluate the effect of particle size on its biosorption efficiency of AFBP for the removal of BPB. The mixture was agitated with 300 mg of each sample, at 200 rpm for 1 h. The dye solution was then decanted and centrifuged at 1,500 rpm for 30 min and the absorbance of the supernatant was then analysed using a UV-Vis spectrophotometer at 590 nm [46, 49].

## 2.6 Biosorption Isotherms

Langmuir and Freundlich isotherm models were used to describe the biosorption isotherm of BPB from aqueous solution by the FBP developed. These isotherms were fitted to the adsorption data and their contacts were evaluated. The correlation coefficient, (R<sup>2</sup>) was used to express the fitness of the experimental data, while the model parameters were evaluated accordingly [50].

### 2.6.1 Langmuir isotherm

The Langmuir model is represented, commonly, as in Eq. (6) and its linear form in Eq. (7). The Langmuir isotherm constants,  $b$ , and  $q_{\max}$  were determined from the plot of  $1/q_e$  versus  $1/C_e$  [51].

$$q_e = \frac{(q_{\max} K_L C_e)}{(1 + K_L C_e)} \quad (6)$$

$$C_e/q_e = C_e/q_{\max} + 1/K_L q_{\max} \quad (7)$$

where,  $q_e$  = Amount of BPB adsorbed at equilibrium (mg/g),  $q_{\max}$  = Maximum AFBP biosorption capacity (mg/g),  $b$  = Langmuir equilibrium constant (L/mg) and  $C_e$  = Equilibrium dye concentration in the solution (mg/L)

### 2.6.1.1 Separation factor

The Separation factor ( $R_L$ ) is a dimensionless constant (Eq. 8) that is incorporated as an important feature in the study of Langmuir isotherm [51]. It is employed to determine the extent of satisfactoriness or otherwise in a batch adsorption system under investigation. Thus, if  $R_L > 1$  then the isotherm is unfavourable,  $R_L = 1$  then the isotherm is linear,  $R_L = 0$  then the isotherm is irreversible, while the condition of  $0 < R_L < 1$  indicates that the isotherm is favourable.

$$R_L = 1/(1 + b C_e) \quad (8)$$

where  $R_L$  is the separation factor,  $b$ , the constant from Langmuir equation, and  $C_e$  the initial dye concentration.

### 2.6.2 Freundlich isotherm

The Freundlich isotherm assumes that the adsorbent surface involved in adsorption study is heterogeneous with its adsorption sites at varying energy levels [52]. Freundlich isotherm model (Eq. 9) was investigated to determine its suitability in understanding the biosorption of BPB onto the AFBP developed. Its linear form is represented as Eq. (10), while the Freundlich isotherm constants,  $K_f$  and  $1/n$ , were determined from the plot of  $\log q_e$  versus  $\log C_e$ .

$$q_e = K_f C_e^{1/n} \quad (9)$$

$$\log q_e = \log K_f + 1/n \log C_e \quad (10)$$

where,  $q_e$  = Amount of sorbate absorbed at equilibrium (mg/g),  $K_f$  = Freundlich constant ((mg/g) (L/mg)<sup>1/n</sup>),  $1/n$  = Freundlich exponent (dimensionless),  $C_e$  = Equilibrium dye concentration in the solution (mg/L) [52].

## 2.7 Biosorption Kinetic Modelling

The sorption kinetics is an important property, which is used to understand the pattern and mechanism of the adsorption process. Common kinetic models include the pseudo-first-order, pseudo-second-order kinetic, and Elovich models [50].

### 2.7.1 Pseudo-first-order model

The pseudo-first-order model is described as in Eq. (11) which is usually integrated with the initial condition that  $q_t = 0$  at  $t = 0$  and its simplification leads to a linear form stated in Eq. (12). The Pseudo first order constants,  $k_1$ , and  $q_e$ , were evaluated from the plot of  $(\log (q_e - q_t))$  versus  $t$ .

$$dq_t/dt = K_1 (q_e - q_t) \quad (11)$$

$$\ln (q_e - q_t) = \ln q_e - K_1 t \quad (12)$$

where,  $q_e$  = Amount of solute absorbed at equilibrium (mg/g),  $q_t$  = Amount of solute absorbed at time  $t$  (mg/g),  $k_1$  = Pseudo first-order equilibrium rate constant (1/min) and  $t$  = Contact time (min)

### 2.7.2 pseudo-second-order model

The pseudo-second-order model is expressed as in Eq. (13) and can be integrated with boundary conditions  $t = 0$  to  $t = t$  and  $q_t = 0$  to  $q_t = q_e$ . Simplifying the integration further would lead to a linear form (Eq. 14) and a linear form was formed (Eq. 14) which will facilitate a linear plot of  $t/q_t$  versus  $t$  to evaluate the Pseudo-second-order constants ( $k_2$  and  $q_e$ ).

$$dq_t/dt = k_2(q_e - q_t)^2 \quad (13)$$

$$t/q_t = 1/k_2 q_e + t/q_e \quad (14)$$

where,  $q_e$  = Amount of solute absorbed at equilibrium (mg/g),  $q_t$  = Amount of solute absorbed at time  $t$  (mg/g),  $k_2$  = Pseudo-second-order equilibrium rate constant (g/mg/min),  $t$  = Contact time (min)

### 2.7.3 Elovich model

The Elovich model equation is given as expressed in Eq. (15) and its linear form is given by Eq. (16). The Elovich coefficients such as initial adsorption rate ( $\alpha$ ), and the desorption constant ( $\beta$ ) were evaluated from the intercept and slope of the straight-line plots of  $q_t$  against  $\ln t$  [53].

$$dq_t/dt = \alpha \exp(-\beta q_t) \quad (15)$$

$$q_t = 1/\beta (\ln \alpha + 1/\beta \ln t) \quad (16)$$

where  $\alpha$  is the initial adsorption rate (mg/g min),  $\beta$  is related to the extent of surface coverage and activation energy for chemisorption (g/mg).

## 2.8 Test of Kinetics Model

The suitability PFO and PSO, to provide insight into the adsorption mechanism that took place between the AFBP developed and the BPB dye in aqueous medium was verified with one of the common error analyses such as the Sum of Error Squares (SSE, %) stated in Eq. (17) [54].

$$\% SSE = \sqrt{(\sum [q_e - q_t]^2) / N} \quad (17)$$

where  $q_{e(\text{exp})}$  = Adsorption capacity at equilibrium experimental (mg/g),  $q_{e(\text{cal})}$  = Adsorption capacity at equilibrium calculated (mg/g) and  $N$  = Number of data point.

## 3. RESULTS AND DISCUSSION

### 3.1 Characteristics of AFBP Developed

The proximate analysis of the biosorbent expressed in terms of moisture content, ash content, volatile matter, and fixed carbons, (Table 1) indicate that ash content of treated flamboyant pods was 31.20% which is lower than the ash content (33.85%) of the untreated FBP. Low ash content is often preferred for effective adsorbent [50]. The lower ash content suggests that the AFBP has improved and better sorbent properties than the untreated. It further indicates that the activation process has improved the property of the raw FBP. However, the ash content (33.85% and 31.20%) observed for untreated and treated FBPs in this study, were higher than 2.80%, 12.87% and 15.73% reported by Seshadri, et al. [37] and Pandimadevi, et al., [23] (Table 1). This development may be attributed to the variations in the composition of different species of flamboyant trees in different regions of the world.



The moisture content of treated flamboyant pods, 9.90% is much higher than that of untreated flamboyant pods, 3.66%. and these values are higher than 0.22% reported by Seshadri, et al., [37] while only the moisture content of the treated flamboyant pods is higher than 5.21% reported by Pandimadevi, et al., [23]. This increase may be due to the treatment processes, particularly, activation where the material was soaked in the activants for a long time and the drying process involved in the study was to constant weight and not to complete dryness.

The fixed carbon (24.90%) of treated flamboyant pods is much higher than that (14.85%) of untreated flamboyant pods and this suggests that it would be more economical to choose AFBP flamboyant pods as the precursor of biosorbent production. The fixed carbon 14.85% and 24.90% for FBP and AFBP, respectively, are higher than 5.20%, 5.95%, 7.40% and 8.30% reported by Seshadri, et al., [37], Hesas, et al., [55], Ponnusami, et al., [56] and Pandimadevi, et al., [23], respectively. The volatile matter (47.64% and 34.00%) observed for FBP and AFBP in this study, were less than 92.03% and 75.97% reported by Seshadri, et al., [37] and Pandimadevi, et al., [23], respectively. This indicates that the volatile matter of the species of flamboyant used in this study is relatively different from the species used in previous studies [52], although not stated.

Table 1: Comparison of the proximate analysis of present work to past work

Biosorbent	Moisture Content (%)	Ash Content (wt. %)	Volatile Matter (wt. %)	Fixed Carbon (%)	References
Flamboyant Pods	0.22	2.80	92.03	5.20	[37]
Flamboyant Pods	5.21	12.87	75.97	5.95	[23]
FBP	3.66	33.85	47.64	14.85	This study
AFBP	9.90	31.20	34.00	24.90	This study

FBP Flamboyant Pods, AFBP Activated Flamboyant Pods

### 3.2 Fourier transforms infrared spectroscopy (FTIR) analysis

The FTIR spectra of both FBP and AFBP biosorbent are shown in Figure 2a-b. The spectrum of the biosorbent was measured within the range of 400-4000  $\text{cm}^{-1}$  wave number. The spectrum of FBP before activation with  $\text{ZnCl}_2$  showed prominent peaks at 3495.3  $\text{cm}^{-1}$  and 2954.6  $\text{cm}^{-1}$  (Figure 2a) that are attributed to O-H stretching and C-H stretching bond of alkyl group respectively. A small peak was noticed at about 2011.0  $\text{cm}^{-1}$  and assigned to the C-H stretching vibration of an alkyl group, and the band at 1710.9  $\text{cm}^{-1}$  is related to the C=O stretching carbonyl group, another band was found at about 1117.5  $\text{cm}^{-1}$ , which is ascribed to C=C stretching alkenes group.



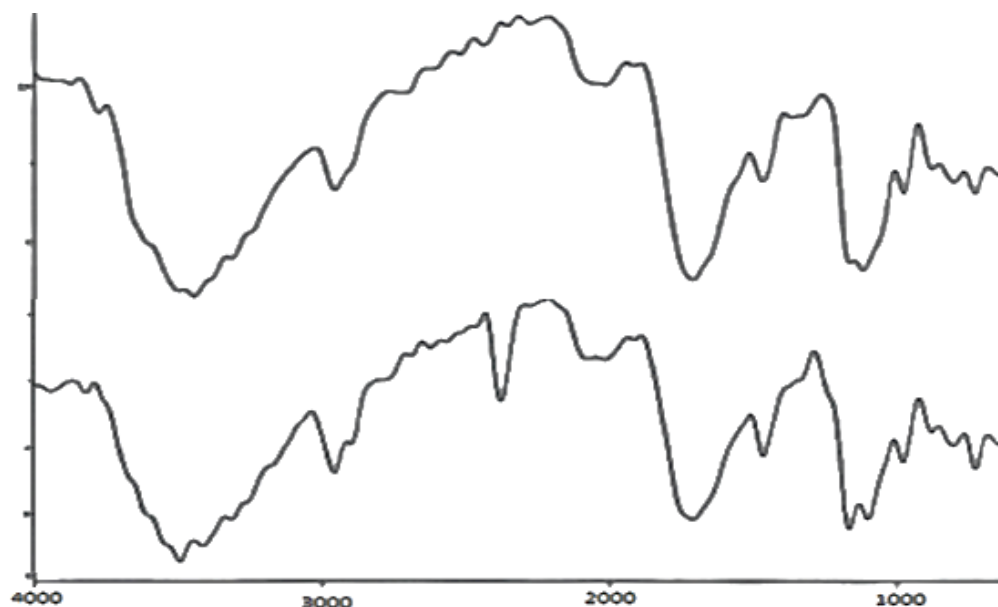


Figure 2: FTIR spectra of (a) untreated and (b) treated flamboyant pods

Some of the peaks were observed in FBP spectra were still present in AFBP after treated with  $\text{ZnCl}_2$ , however, there were some changes in their wavenumbers (Figure 2b), indicating that the activant have interacted chemically with the flamboyant pod. The prominent peak that appears at about  $3495.3 \text{ cm}^{-1}$  was reduced to  $3485.7 \text{ cm}^{-1}$  and the peak of the C-H stretching alkyl group was decreased from  $1710.9 \text{ cm}^{-1}$  to  $1710.1 \text{ cm}^{-1}$ . The peak  $1117.5 \text{ cm}^{-1}$  of the C=C band was decreased to  $1101.0 \text{ cm}^{-1}$  which is an indication that a new peak has been formed and it is related to N-H bending of amide group and this is predicting that the functional groups have responsibility for the electrostatic attraction of zinc chloride cations onto flamboyant pod powder [57].

### 3.3 Effect of Various Parameters on Removal of Bromophenol Blue Dye

#### 3.3.1 Effect of initial dye concentrations on biosorption

The change in adsorption capacity and percentage removal with varying initial concentration (Figure 3a-b), respectively, indicates the highest adsorption capacity of  $7.5762 \text{ mg/g}$  and highest removal efficiency of  $75.7627\%$  were observed at the higher concentration of  $30.0 \text{ mg/L}$  while their lowest values  $0.7458 \text{ mg/g}$  and  $44.7458\%$  were recorded at  $5 \text{ mg/L}$ . These values increased as the concentration increased as expected of the adsorbent [50].

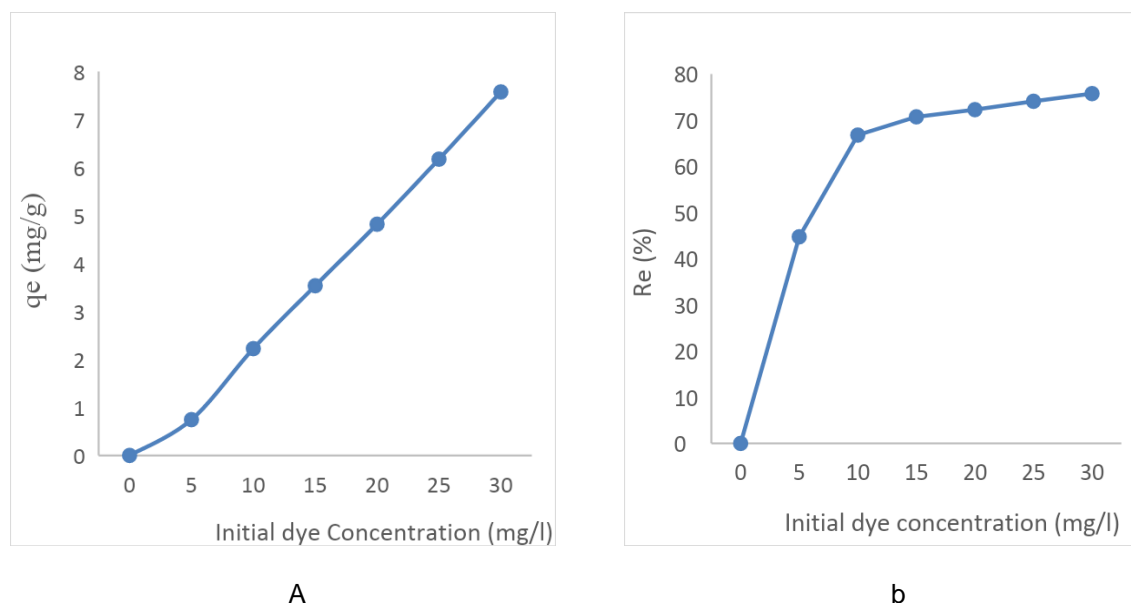
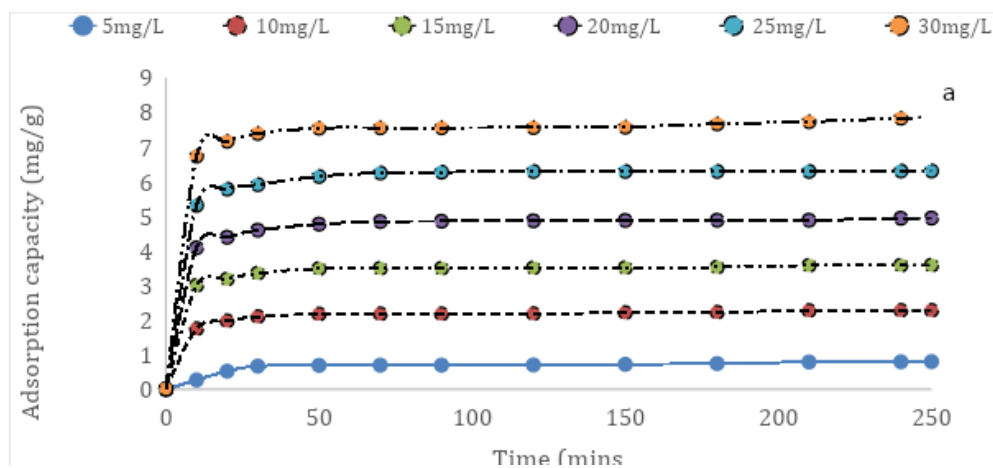


Figure 3: Plot of (a) Adsorption capacity and (b) Removal efficiency against initial dye concentration

Previous research has shown that increase in initial concentration influences biosorption capacity ( $q_e$ ) higher  $q_e$  and the works of Senthilkumar, et al., [58], as well as Murali and Uma, [59], have reported a similar trend. The actual amount of bromophenol blue dye adsorbed per unit mass of biosorbent increased with an increase in dye concentration. This phenomenon can be explained in terms of available active sites. It may be suggested that the initial concentration of BPB provided substantial during force which effectively overcomes mass transfer resistance of the dye solute between the solids and aqueous phase. Thus, at higher initial concentrations, there is a high density of BPB on the surface of AFBP and this led to high adsorption tendency [60, 61].

### 3.3.2 Effect of contact time on biosorption

The maximum adsorption capacity obtained for 5, 10, 15, 20, 25 and 30 mg/L of BPB were 0.79, 2.28, 3.58, 4.94, 6.31 and 7.89 mg/g, respectively (Figure 4a). The corresponding maximum removal efficiency were 47.80%, 68.31%, 71.64%, 74.15%, 75.66% and 78.42% as the time increased from 10 to 270 min (Figure 4b).



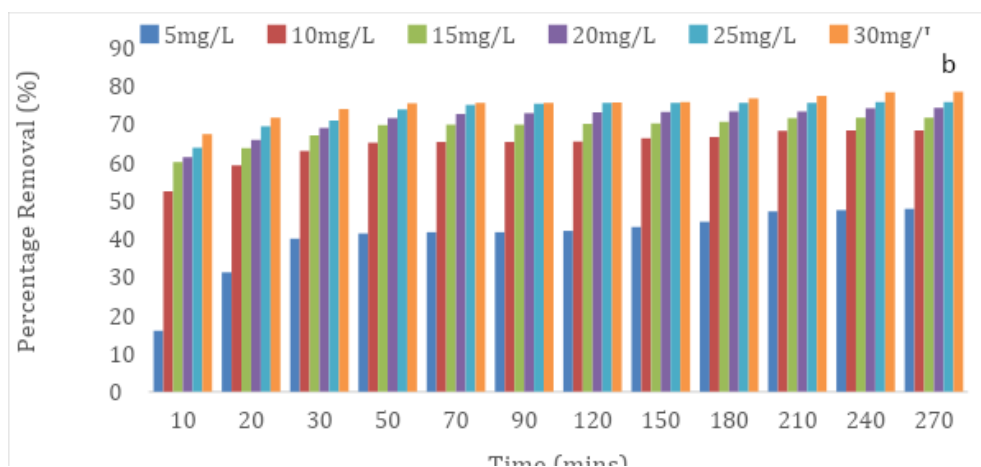


Figure 4: Plot of (a) adsorption capacity and (b) Removal efficiency against time

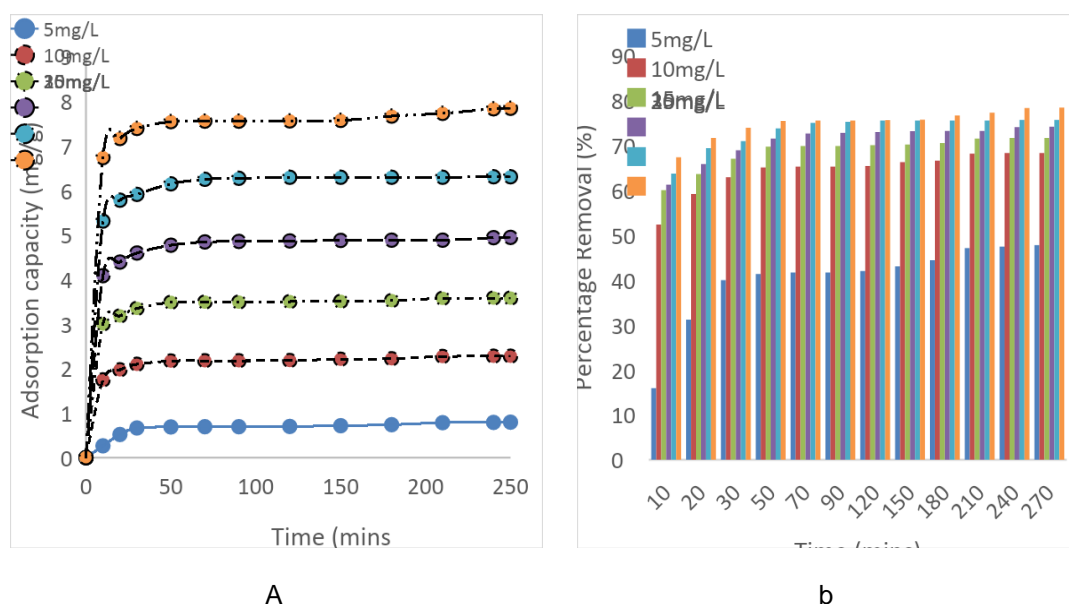


Figure 4: Plot of (a) adsorption capacity and (b) Removal efficiency against time

The extent of dye removed by AFBP was found to increase with the increased contact time. The removal of dye by adsorption using AFBP was found to be rapid at the initial period of contact and then become slower with the increasing contact time and this may be due to the strong attractive forces between the dye molecules and the biosorbent at the beginning [62]. Where the active sites were not occupied. However, the trend became slower due to less available sites, thus at a later time, the rate of adsorption became slower with increasing time.

The changes in the rate of removal with time might be because initially all biosorbent sites were vacant and the solute concentration gradient was high [63]. A similar trend was reported by Khalifa, et al., [64] and Pandimadevi, et al., [23] for the adsorption of methylene blue onto jute fibre carbon. Theoretically, during adsorption of dyes, initially, the dye molecules will move to the boundary layer of the adsorbent before they then diffuse into the adsorbent surface and subsequently, into the porous structure of the

adsorbent. This phenomenon represents the rapid, moderate, and slow regimes displayed in this study [65].

### 3.3.3 Effect of biosorbent dosage on biosorption

The effect of biosorbent dosage (0.1-0.7 g) on the adsorption capacity and removal efficiency of the AFBP for removal of BPB from aqueous solution indicates that the highest adsorption capacity and removal efficiencies were 6.09 mg/g and 87.20%, respectively. The adsorption capacity of the activated flamboyant pods (AFBP) for removal of BPB increases with increasing the loading from 0.1-0.5 g (Figures 5a-b). Indeed, the total number of active sites increased with increasing biosorbent dosage and this influenced the adsorption trend. The amount of BPB adsorbed per unit mass of AFPB decreased from 6.09 to 2.49 mg/g as the dosage increased, due to a decrease in the solute transfer rate onto the surface of the adsorbent and availability of more active sites [57].

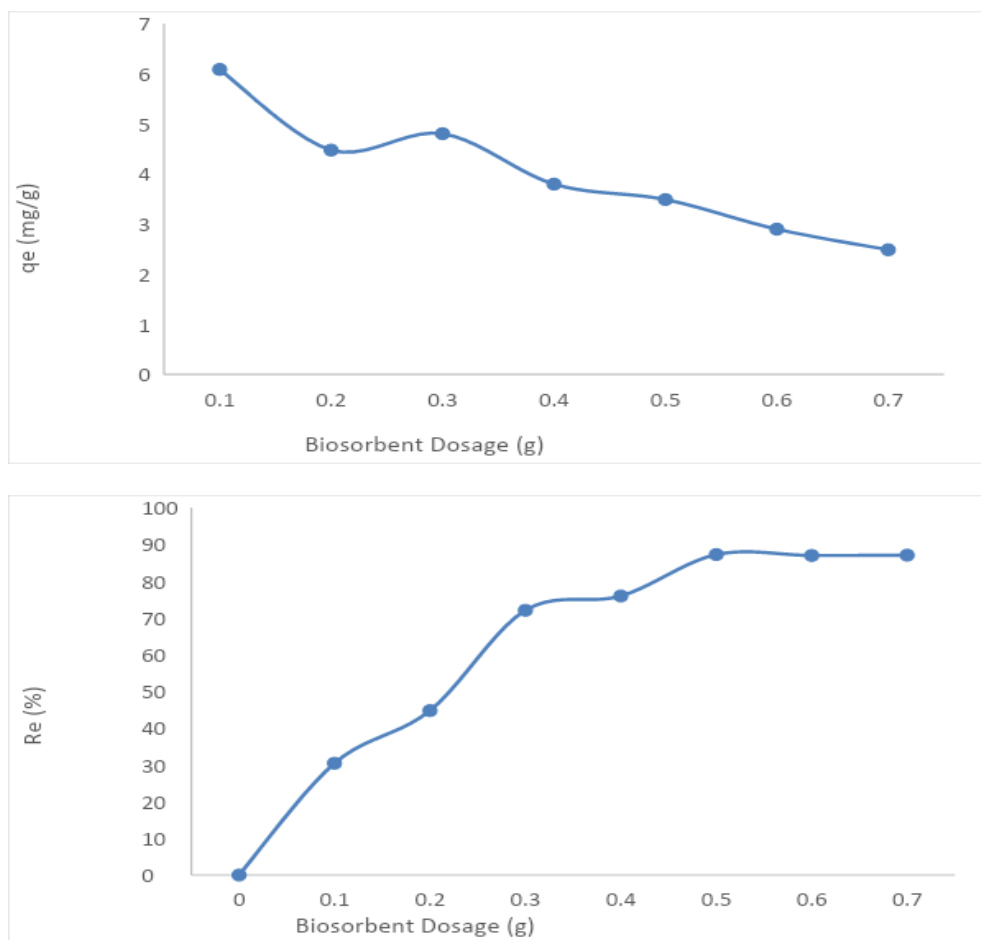


Figure 5: Graph of (a) Adsorption capacity and (b) Removal efficiency against biosorbent dosage

### 3.3.4 Effect of particle size on biosorption

Available surface area, which is an important controlling parameter in the adsorption process. It is inversely related to the particle size of a given biosorbent. The effects of particle size (850, 425, and 300  $\mu\text{m}$ ) were investigated in this study. It was established that adsorption of BPB increased with decrease in particle size of AFBP that is, the removal efficiency for 850, 425, and 300  $\mu\text{m}$  were 54.90, 72.71 and 86.70%, (Figure 6) this is because smaller particles have more surface area and this provides access to

more pores in the particles. It is also believed that the breaking up of large particles to form smaller ones opens some tiny sealed channels, which might then become available for adsorption. Consequently, the sorption is often higher in adsorbent with smaller particle sizes than those with larger particle sizes. These findings are consistent with the reported of Asfaram, et al., [66] and Wanyonyi, et al., [67] for the removal of Direct Red 12B using Garlic peel and Congo Red on *E. Crassipe* roots, respectively. This relationship supports the choice of powdered adsorbent over granulated one in adsorption studies.

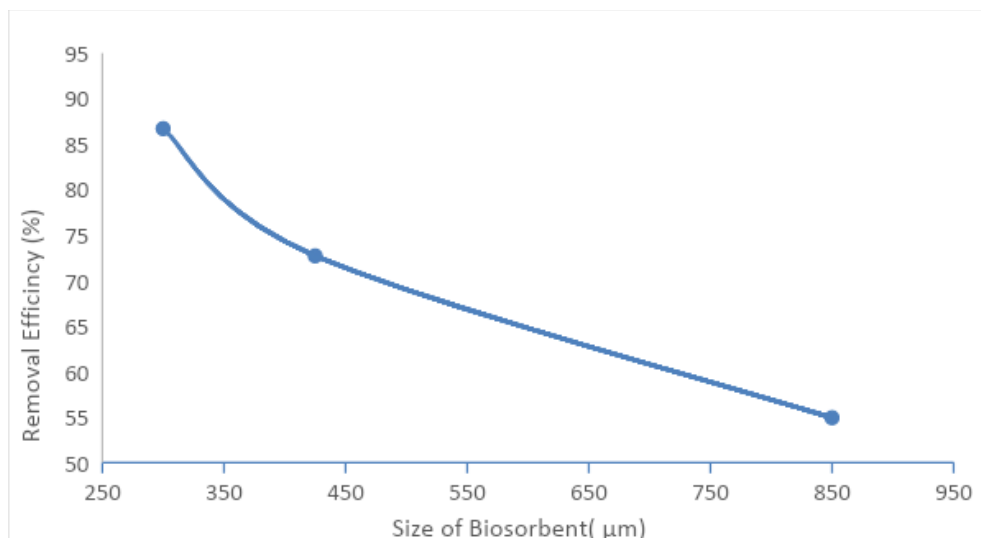
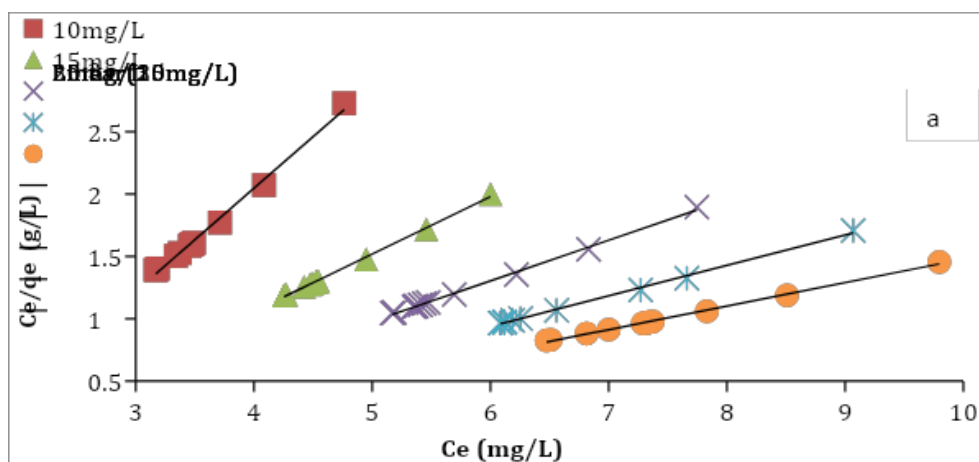


Figure 6 Graph of particle size effect of AFBP on the removal of BPB

### 3.4 Isotherm Parameters for Biosorption of BPB onto AFBP

The biosorption isotherm of BPB removal by using AFBP at different initial dye concentrations was studied using the Langmuir and Freundlich models (Figures 7a-b). The monolayer capacity  $q_m$  obtained from the plot of Langmuir isotherms (Figures 7a) are 1.2092, 2.1730, 3.0684, 4.0933, and 5.3079 mg/g for 10, 15, 20, 25 and 30 mg/L concentration (Table 2). Langmuir constant  $b$  and  $q_{max}$  are 0.4636-0.6559 and 1.2092-5.3079, respectively while Freundlich constant  $K$  and  $1/n$  were in the range 4.7973-15.5382 and 0.3631-0.6387, respectively.



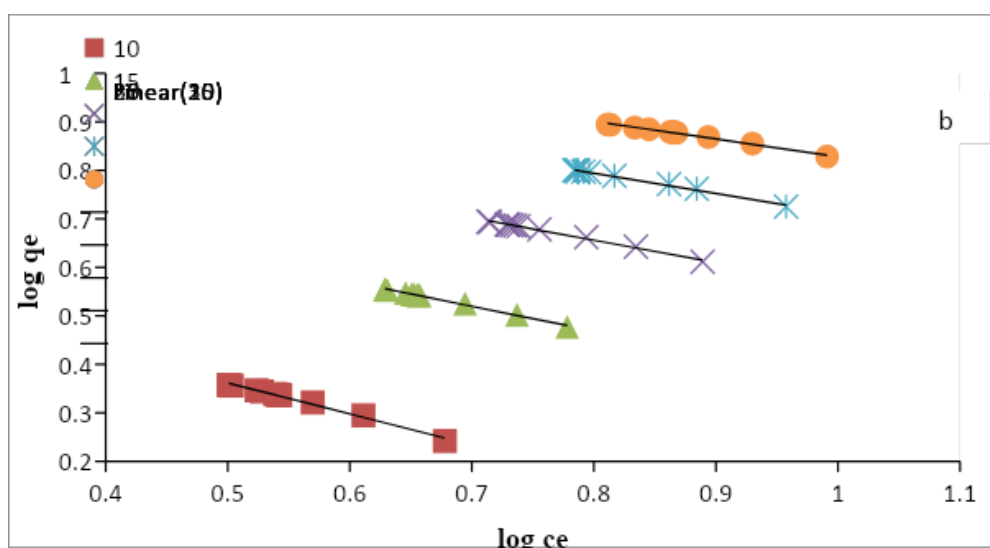
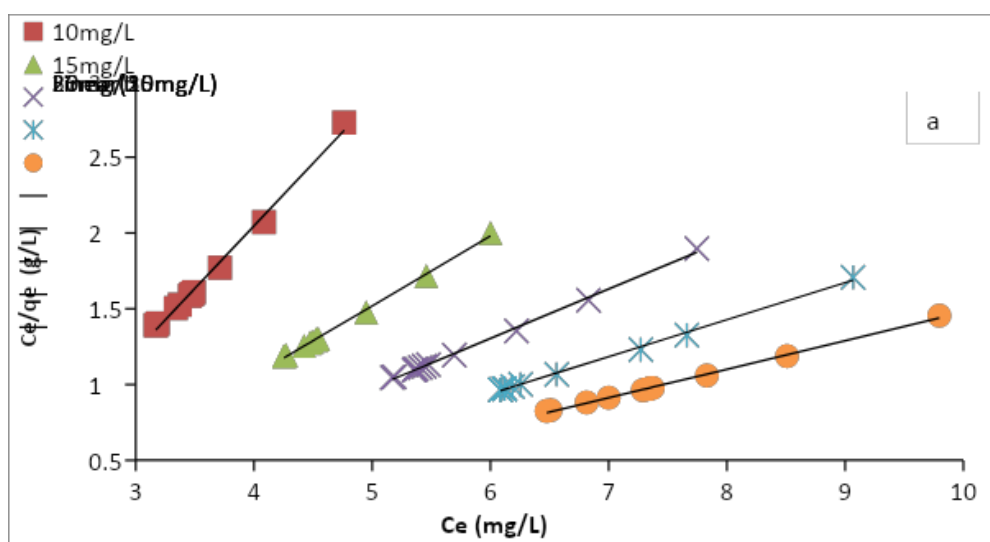
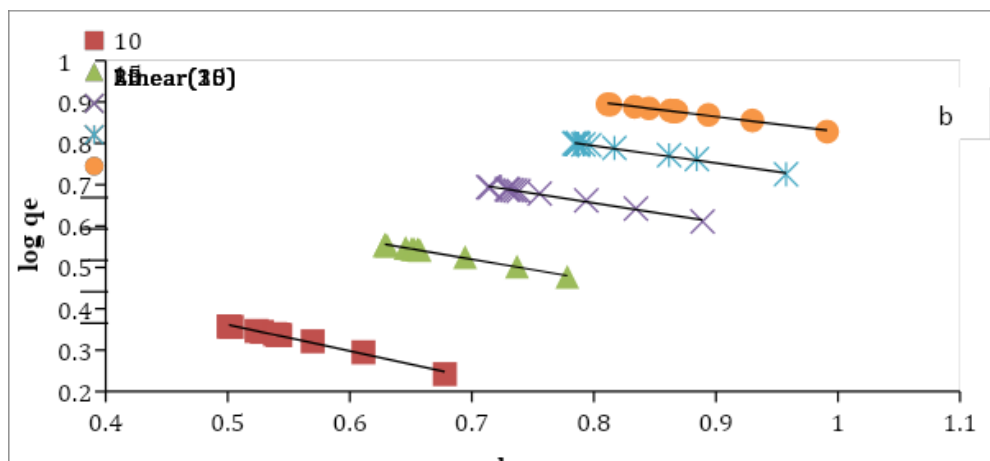


Figure 7: (a) Langmuir and (b) Freundlich isotherm model plot for biosorption of BPB dye onto AFBP

Table 2 Langmuir and Freundlich isotherm model constants for adsorption of BPB onto AFBP

Conc. (mg/l)	Langmuir isotherm				Freundlich isotherm		
	$q_m$ (mg/g)	b	$R_L$	$R^2$	n	$K_f$ (mg/g)(L/mg) <sup>1/n</sup>	$R^2$
10.00	1.2092	0.6559	0.1323	0.9938	2.754	15.5382	0.9911
15.00	2.1730	0.5888	0.1017	0.9979	2.406	13.3844	0.9938
20.00	3.0684	0.5004	0.0908	0.9975	2.162	10.6170	0.9941
25.00	4.0933	0.4641	0.0794	0.9977	1.971	7.4955	0.9953
30.00	5.3079	0.4636	0.0671	0.9976	1.566	4.7973	0.9895

The overall trend obtained for the Langmuir separation factor,  $R_L$ , and the Freundlich exponent ( $1/n$ ), are below one for all the concentration ranges studied, representing favourable adsorption processes. A similar trend for  $R_L$  and  $1/n$  were observed for methylene blue and brilliant green dyes removal from aqueous solution using agricultural wastes activated carbon [68]. This showed good linearity for the Langmuir and Freundlich isotherm, constants are valid and this supports the applicability of the isotherms. A similar observation was reported for the adsorption of malachite green on degreased coffee beans [69]. The correlation coefficients, ( $R^2$ ) values of Langmuir and Freundlich isotherms are in the range of 0.9938-0.9979 and 0.9895-0.9953, (Table 2) respectively. These  $R^2$  values described the fitness of the model for the set of observations. This study indicates that Langmuir isotherm was a better fit for the adsorption data of BPB than Freundlich isotherm, and based on the  $R^2$  value.

The Freundlich the exponent (n), known as heterogeneity factor, is in range of 1.566-2.754, which falls within the ranges of 1 to 10 and this indicates favourability of the adsorption as well as advantageous adsorption [70]. Value of 'n' tending towards 10 displays a higher degree of homogeneity of the particle surface [71]. The lower the value 'n' in this study signifies that the surface characteristics may involve more than a homogenous surface. The Langmuir model assumes monolayer coverage and constant adsorption energy while the Freundlich equation deals with heterogeneous surface adsorption. The applicability of both Langmuir and Freundlich isotherms to the studied system implies that both monolayer sorption and heterogeneous surface conditions exist under the used experimental conditions.

The essential characteristics of the Langmuir isotherms can be described by a separation factor,  $R_L$ . The value of separation factor ( $R_L$ ) indicates the nature of the absorption process [72]. The values of  $R_L$  for initial dye concentrations from 10 to 30 mg/L were found to range from 0.1323 to 0.0671. The  $R_L$  values indicate that adsorption is more favorable for the bromophenol blue/activated flamboyant pod biosorbent system. A similar range was reported by Pandimadevi, et al., [23], for the adsorption of methylene blue from aqueous solution onto activated carbon prepared from Flamboyant pods by chemical activation with  $H_2SO_4$ .

### 3.5 Kinetics of Study

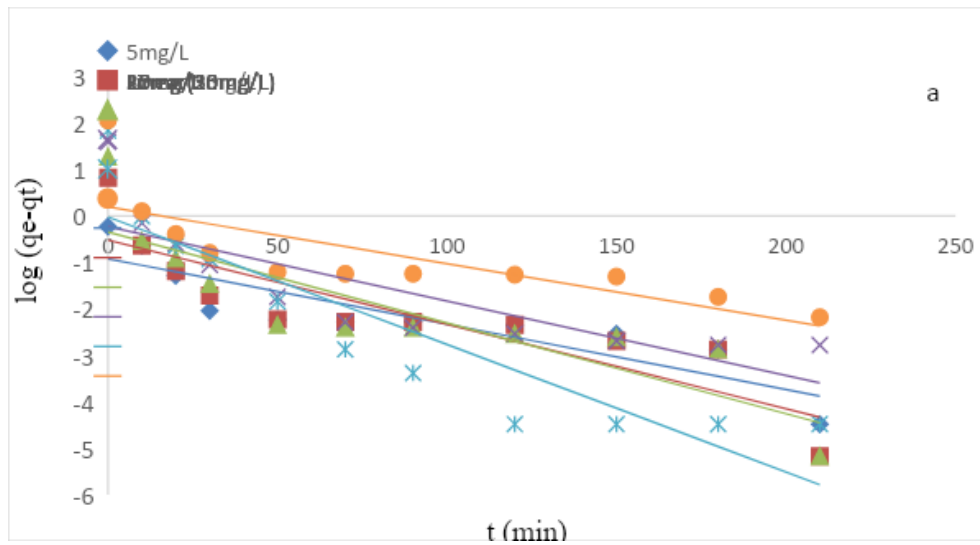
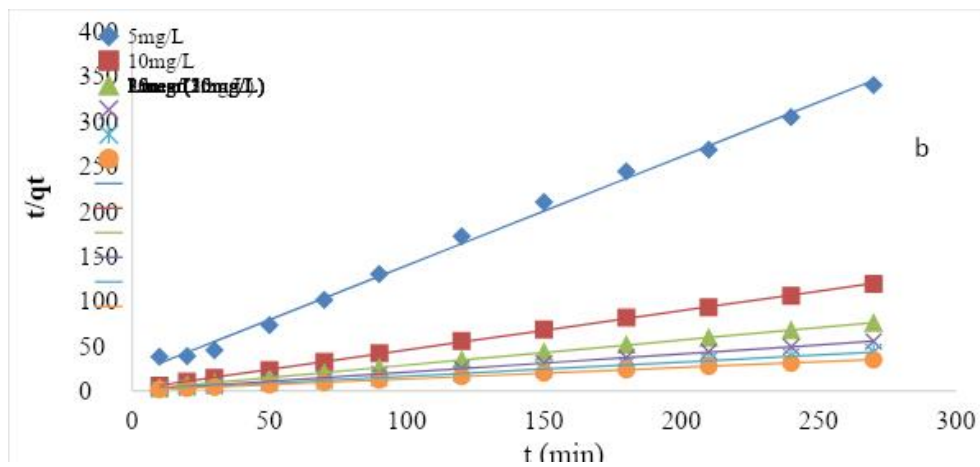
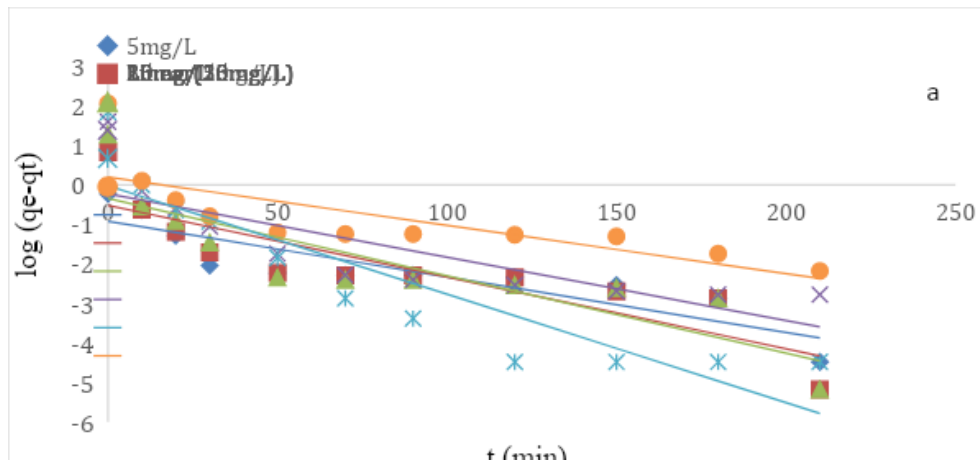
The three common kinetic models applied to fit the experimental data obtained for BPB adsorption by AFBP are Pseudo first order (PFO), Pseudo second-order (PSO), and Elovich models.

#### 3.5.1 Pseudo-first-order model

The intercepts and the slope of the plots of  $\log(q_e - q_t)$  versus  $t$  (Figure 8a). were used to determine the amount of BPB adsorbed onto AFBP at a different time is the  $q_t$  (mg/g), and at the equilibrium, the amount of bromophenol blue adsorbed onto activated flamboyant pod is  $q_e$  (mg/g). The values obtained for  $k_1$  were 0.0141, 0.0181, 0.0196, 0.0160, 0.0275 and 0.0122 min<sup>-1</sup> for 5, 10, 15, 20, 25 and 30 mg/L while their corresponding  $q_e$  were 0.3980, 0.5944, 0.7077, 0.7960, 0.9789 and 0.8233 mg/g, respectively, (Table 3). The experimental equilibrium data ( $q_e$ ) (0.7912-7.9970) were not matched with the calculated equilibrium ( $q_{e_{cal}}$ ) (0.3980-0.8233) for the pseudo-first-order kinetics. Their  $R^2$  values (0.7912, 0.7657,



0.7518, 0.6760, 0.8150, and 0.5931) are relatively low and thus suggest that this model, due to the poor fitness of the adsorption data, cannot elucidate the adsorption process.



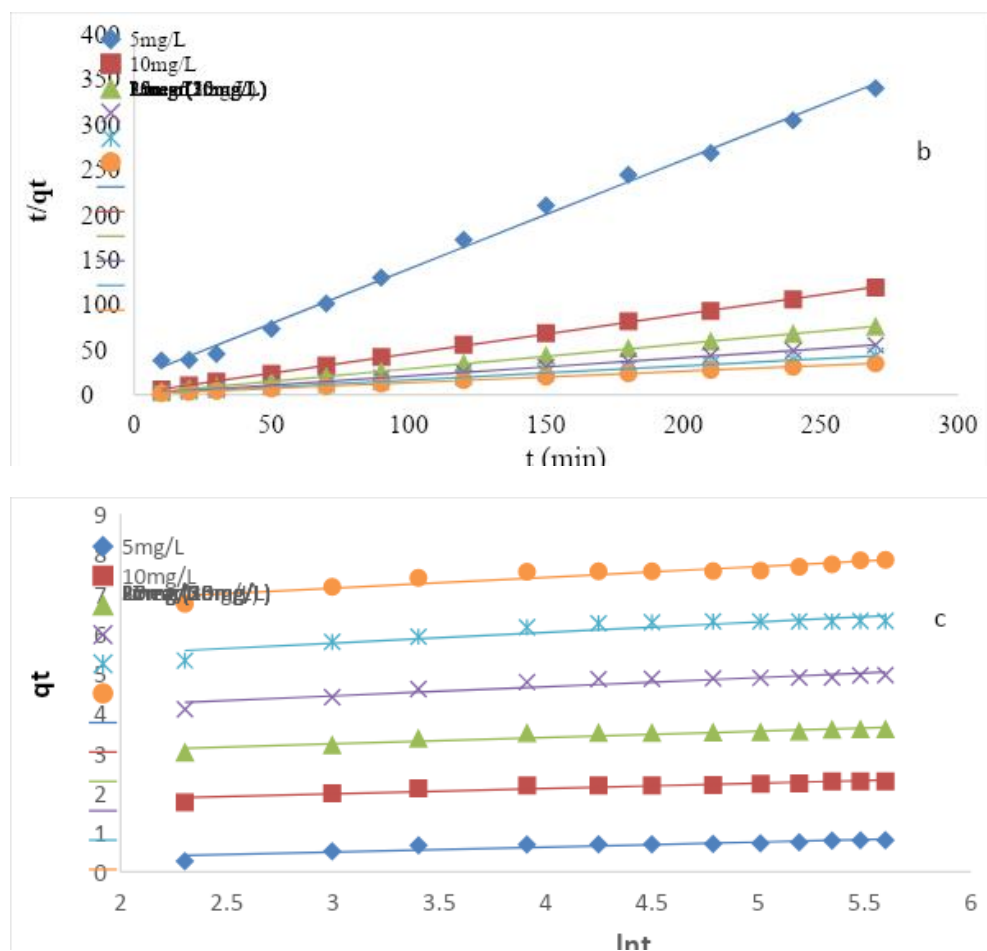


Figure 8: Plot of (a) Pseudo-first-order, (b) pseudo-second-order and (c) Elovich kinetic model for the biosorption of BPB dye onto the AFBP

### 3.5.2 pseudo-second-order model

The plotting of  $t/q_t$  versus  $t$  (Figure 8b). was used to evaluate the intercept ( $1/k_2 q_e^2$ ) and slope ( $1/q_e$ ) of the Lagergren (pseudo-second-order) model equation. The values of model parameters ( $k_2$ ,  $h$ ,  $q_e$  and  $R^2$ ) at different concentration were in the ranges 0.0450-0.1075, 0.0545-3.8183, 0.8290-7.8550, and 0.9961-1.000, respectively. The values of  $R^2$ ,  $h$ , and  $q_{e(crit)}$  increased, generally, with increased BPB concentration but dropped for the last concentrations (30 mg/l) which may suggest that desorption is about to set in at that condition. Similar kinetics was also observed in adsorption of methylene blue on papaya seeds [73] and adsorption of Congo red dye on cattail root [74].

### 3.5.3 Elovich model

The Elovich coefficients evaluated from the plot of  $q_t$  versus  $\ln t$  based on the experimental data (Figure 8c). The initial adsorption rate, ( $\alpha$ ) and the extent of surface characteristics coverage ( $\beta$ ) were calculated as the intercept and slope of the straight-line plots obtained. The values of  $R^2$  were 0.8046, 0.8642, 0.8702, 0.8663, 0.8306 and 0.8828 for 5, 10, 15, 20, 25 and 30 mg/L. The  $R^2$  is within the acceptable ranges (0.7500-1.000) suitable to the kinetics of BPB dye adsorption on adsorbent [56]. The values of  $\alpha$  increased from 0.1253 to 0.2722 while values of  $\beta$  increased from 2.6224 to  $1.2 \times 10^{10}$ , as the concentration

increased from 5 to 30 mg/l. However, these values were comparatively lower than the corresponding  $R^2$  obtained for PFO and PSO. The Elovich model is not as suitable as expected for this study.

Table 3: The summary of the three common kinetic models applied to fit the experimental results of BPB adsorption by AFBP

Conc. mg/L	$q_{e(exp)}$ (mg/g)	Pseudo first-order			pseudo second-order				Elovich		
		$K_1$	$q_{e(cal)}$	$R^2$	$q_{e(cal)}$	$h = (k_2 q_e^2)$	$K_2$	$R^2$	$\alpha$	$\beta$	$R^2$
5.00	0.796	0.014	0.398	0.791	0.829	0.054	0.079	0.996	0.125	2.6224	0.804
	1	1	0	2	0	5	2	2	3		6
10.00	2.276	0.018	0.594	0.765	2.299	0.568	0.107	0.999	0.134	11,068	0.864
	9	1	4	7	9	4	5	7	1		2
15.00	3.819	0.019	0.707	0.751	3.607	1.380	0.106	0.999	0.157	3.7E+0	0.870
	0	6	7	8	5	5	1	9	6	7	2
20.00	4.943	0.016	0.796	0.676	4.970	2.057	0.083	0.999	0.230	1.1E+0	0.866
	0	0	0	0	0	6	3	9	2	7	3
25.00	6.305	0.027	0.978	0.815	6.353	3.818	0.094	1.000	0.265	1.2E+0	0.830
	1	5	9	0	0	3	6	0	7	8	6
30.00	7.897	0.012	0.823	0.593	7.855	2.777	0.045	0.999	0.272	1.2E+1	0.882
	0	2	3	1	0	8	0	7	2	0	8

### 3.6 Test of Kinetic Models

The percentage sum of error squares (%SSE) and correlation coefficient ( $R^2$ ) was used to determine the suitability of either pseudo-first-order and pseudo-second-order kinetic models for any adsorption system. Higher the  $R^2$  and lower values of %SSE suggest the goodness of the fit for the experimental data, thus, data set with least %SSE is accepted for a given model [19]. %SSE obtained were in the range of 0.1585-50.0368 and 0.0005-0.0023 for the PFO and PSO, respectively. The calculated adsorption capacity ( $q_{e(cal)}$ ) for PSO is closer to the experimental results and its %SSE value is lower compared to that of pseudo-first-order. This substantiates further, that the PSO kinetic equation could best describe the adsorption kinetics of BPB on the AFBP biosorbent. Lastly, based on the  $R^2$  the order of fitness/suitability of the models is pseudo-second-order > Elovich > pseudo-first-order.

## 4. CONCLUSION

Removal of bromophenol blue from dye aqueous solution was carried out using activated flamboyant pod biosorbent prepared from the agricultural residue (flamboyant pod) under the influence of various adsorption factors. The influence  $ZnCl_2$ , chemical activant, influenced the activation process as evident in the reduced ash content and adjusted functional groups on the surface of the flamboyant pod. Maximum adsorption capacity and removal efficiency obtained for 5-30 mg/L of BPB in the range of 0.79-7.89 mg/g and 47.80-8.42%, respectively. The two adsorption isotherms (Langmuir and Freundlich) isotherm explained the biosorption of BPB onto AFBP due to the heterogeneous and homogeneous surface

characteristics of the adsorbent. The sorption kinetics of the system is well suited to pseudo-second-order at the expense of pseudo-first-order and Elovich kinetic models, while the order of fitness/suitability of the models is pseudo-second-order > Elovich > pseudo-first-order. Considering the data and analysis presented in this study, it is suggested that flamboyant pod is promising biomass for the remediation of dye-bearing industrial effluents.

**ETHICAL APPROVAL:** Not applicable, no ethical issues.

## REFERENCES

1. Emenike PC, Omole DO, Ngene BU, Tenebe IT. Potentiality of agricultural adsorbent for the sequestering of metal ions. *Global J. Environ. Sci. Manage.* 2016;2(4):411-442
2. Haffad H, Zbair M, Anfar Z, Ahsaine HA, Bouhlal H, Khallok H. Removal of Reactive Red-198 Dye Using Chitosan as an Adsorbent: Optimization by Central Composite Design Coupled with Response Surface Methodology. *Tox. Reviews.* 2019;DOI:10.1080/15569543.2019.1584822
3. Aghdasinia H, Asiabi HR. Adsorption of a cationic dye (methylene blue) by Iranian natural clays from aqueous solutions: equilibrium, kinetic and thermodynamic study. *Environ. Earth Sci.* 2018;77:218-225
4. Gedam VV, Raut P, Chahande A, Pathak P. Kinetic, thermodynamics and equilibrium studies on the removal of Congo red dye using activated teak leaf powder. *Applied Wat. Sci.* 2019;9:55-63
5. Etim UJ, Umoren SA, Eduok UM. Coconut coir dust as a low cost adsorbent for the removal of cationic dye from aqueous solution. *J. Saudi Chem. Soc.* 2016;20(1):67-76
6. Choi H-J, Yu S-W. Biosorption of methylene blue from aqueous solution by agricultural bioadsorbent corncob. *Environ. Eng. Res.* 2019;24(1):99-106
7. Kannanmarikani U, Sangareswari K, Rajarathinam K. Assessment of dyeing properties and quality parameters of natural dye extracted from *Lawsonia inermis*. *Europ. J. Exp. Bio.* 2015;5(7):62-70
8. Swelam AA, Awad MB, Salem AM. Kinetics Study on the Removal of Cu(II) from Aqueous Solution using Raw and Modified Pumpkin Seed Hulls-Low Cost Biosorbents. *Int. J. Environ.* 2015;4(1):38-50
9. Itodo AU, Oketunde FK. Activated Carbon: Spent, Regenerated, and Reuse for Synthetic Dyestuff Effluent Decolorization. *Int. J. Env. Monit. Prot.* 2017;4(4):29-37
10. Rehman A, Ilyas S, Sultan S. Decolourization and degradation of azo Dye, Synozol Red HF6BN, by *Pleurotus ostreatus*. *Afr. J. Biotech.* 2012;11(88):15422-15429
11. Donghee P, Yeoung-Sang Y, Jong MP. The Past, Present, and Future Trends of Biosorption. *Biotech. Bioproc. Eng.* 2010;15(1):86-102
12. Aremu MO, Alade AO, Araromi DO, Bello A. Optimization of Process Parameters for the Carbonization of Flamboyant Pod Bark (*Delonix Regia*). *Europ. Sci. Jour.* 2017;13(24):165-179
13. Ramesh K, Rajappa A, Nandhakumar V. Adsorption of Methylene Blue onto Microwave Assisted Zinc Chloride Activated Carbon Prepared from *Delonix Regia* Pods - Isotherm and Thermodynamic Studies. *Res. J. Chem. Sci.* 2014;4(7):36-42.
14. Terdputtakun A, Arqueropanyo O, Sooksamiti P, Janhom S, Naksata W. Adsorption isotherm models and error analysis for single and binary adsorption of Cd(II) and Zn(II) using leonardite as adsorbent. *Env. Earth Sci.* 2017;76:777-787
15. Massoudi FM, Etorki A. The use of peanut hull for the adsorption of colour from aqueous dye solutions and dye textile effluent. *Orient. J. Chem.* 2011;27(3):875-884.
16. Mane R, Bhusari VN. Removal of Colour (dyes) from textile effluent by adsorption using Orange and Banana peel. *Int. J. Eng. Res. Appl.* 2011;2(3):1997-2004.
17. Hameed BH, Foo KY, Njoku VO. Microwave-assisted preparation of pumpkin seed hull activated carbon and its application for the adsorptive removal of 2,4-dichlorophenoxyacetic acid. *The Chem. Eng. Jour.* 2013;215-216:383-388
18. Ncibi MC, Mohjoub B, Ouhaibi K. Valorisation of *Posidonia oceanica* leaf sheaths in removing synthetic dye from aqueous media using dynamic column system. *Int. J. Environ. and Waste Manag.* 2014;4:1-22
19. Rajasulochana P, Preethy V. Comparison on efficiency of various techniques in treatment of waste and sewage water – A comprehensive review. *Res.-Efficient Technol.* 2016;2(4):175-184

20. Alade AO, Amuda OS, Afolabi TJ, Okoya AA. Adsorption of naphthalene onto activated carbons derived from milk bush kernel shell and flamboyant pod. *J. Environ. Chem. and Ecotoxico.* 2012;4(7):124-132
21. Abulude FO, Adejayan AW. Nutritional values of flamboyant (*Delonix regia*) seeds obtained in Akure, Nigeria. *Sci. and Edu. Develop.* 2017;1(4):1-18
22. Fahd K. *Landscape Plants: Manual of Sriyadh Plants.* (Vol. 1). Saudi Arabia: High Commission for the development of Arriyadh. 2014.
23. Pandimadevi M, Rajalekshmi G, Mrithaa T, Viji CS. Preparation and Characterisation of Activated Carbon from *Delonix Regia* Seeds for the Removal of Methylene Blue Dye. *J. Indust. Poll. Contr.* 2016;32(2):572-579
24. Mithun M, Gangadware MV, Jadha V. Removal of Methylene Blue from Wastewater by using *Delonix Regia* Seed Powder as Adsorbent. *Int. J. Sci. Eng. and Techn. Res.* 2016; 5(6):2278–7798
25. Adebisi SA, Amuda OS, Adejumo AL, Olayiwola AO, Farombi AG. Equilibrium, Kinetic, and Thermodynamic Studies of Adsorption of Aniline Blue from Aqueous Media Using Steam-Activated Carbon Prepared from *Delonix regia* Pod. *J. Wat. Res. Protect.* 2015;7:1221-1233
26. Syed S, Daniel S, Indhumathi P. Utilising the Pods of *Delonix regia* Activated Carbon for the Removal of Mercury (II) by Adsorption Technique. *Int. J. Res. Chem. Environ.* 2013;3(1):60-65
27. Owoyokun TO, Soile OO, Gayawan E. Chemometric analysis of the effects of initial concentrations, contact time, and temperature on the adsorption capacity of Flamboyant tree (*Delonix regia*) pod. *Int. J. Sci. Eng Res.* 2013;4(3):1-10
28. Sugumaran P, Priya SP, Ravichandran S. Production and Characterization of Activated Carbon from Banana Empty Fruit Bunch and *Delonix regia* Fruit Pod. *J. Sustain. Energy Environ.* 2012;3:125-132
29. Jimoh OT, Iyaka AY, Nubaye M. Sorption Study of Co (II), Cu(II), and Pb(II) ions Removal from Aqueous Solution by Adsorption on Flamboyant Flower (*Delonix Regia*). *Am. J. Chem..* 2012;2(3):165-170
30. Solairaj D, Palanivel R, Srinivasan P. Adsorption of Methylene Blue, Bromophenol Blue, and Coomassie Brilliant Blue by  $\alpha$ -Chitin Nanoparticles. *J. Adv. Res..* 2015;27(1):1-11
31. Okoye CC, Okey-Onyesolu CF, Chime DC, Achike CC. Adsorptive Removal of Bromophenol Blue Dye from Aqueous Solution using Acid Activated Clay. *Int. J. Sci. Res. Manage..* 2018;6(3):2321-3418
32. Ch A, Raju K, Satyanandam. Sorption of Synthetic Bromo Phenol Blue Dye using *Gelidium Cartilagineum* Powder and Optimization using Central Composite Design. *Int. J. Emerg. Eng. Res. Techn.* 2015;3(12):109-127
33. El-Dars F, Shalabi ME, Farag HA, Ibrahim HM, Abdelwahhab MZ. Adsorption Kinetics of Bromophenol Blue and Eriochrome Black T using Bentonite Carbon Composite Material. *Int. J. Sci. Eng. Res..* 2015;6(5):1-14
34. Mashkour MS. Decolorization of Bromophenol blue Dye Under UV- Radiation with ZnO as Catalyst. *Iraq. Nat. J. Chem.* 2012;46:189-198
35. Aadil A, Shahzad M, Kashif S, Muhammad M, Rabia A, Saba A. Comparative Study of Adsorptive Removal of Congo Red and Brilliant Green Dyes from Water Using Peanut Shell. *Middle-East J. Sci. Res.* 2012;11(6):828-832
36. Changying J, Talpur MA, Chandio FA, Junejo SA, Mari IA. Application of oven drying method on moisture content of ungrounded and grounded (long and short) rice for storage. *J. Stored Prod. Postharvest Res.* 2011;2(12):245-247
37. Seshadri S, Sugumaran P, Priya SV, Ravichandran P. Production and Characterization of Activated Carbon from Banana Empty Fruit Bunch and *Delonix regia* Fruit Pod. *J. Sust. Energy Environ.* 2012;3:125-132
38. Jeandson C, Roberta N, Marcio AM, Dênia M. The oven-drying method for determination of water content in Brazil nut. *Biosci. Journ.* 2018;34(3):595-602
39. Feng Y, Yang W, Chu W. Contribution of Ash Content Related to Methane Adsorption Behaviors of Bituminous Coals. *Int. J. Chem. Eng..* 2015;1:1-11
40. Farah JY, El-Gendy NS. Performance, kinetics, and equilibrium in biosorption of anionic dye Acid Red 14 by the waste biomass of *Saccharomyces cerevisiae* as a low-cost biosorbent. *Turk. J. of Eng. Environ. Sci.* 2013;37:146-161
41. Ibrahim MF, Abdelgadir AY. Effect of Growth Rate on Fixed Carbon, Volatile Matter, and Ash Content of *Eucalyptus camaldulensis* Wood of Coppice Origin Grown in White Nile State, Sudan. *J. Forest Prod. Indust.* 2014;3(6):229-235

42. Udoh AU, Duygu D, Ozer T, Akbulut A, Erkaya I, Yildiz K. Fourier transform infrared (FTIR) spectroscopy for identification of *Chlorella Vulgaris* Beijerinck 1890 and *Scenedesmus obliquus* (Turpin) Kützing 1833. *Afr. J. Biotech.* 2012;11(16):3817-3824
43. George ZK, Jie F, Kostas AM. New Biosorbent Materials: Selectivity and BioEng. Insights. *Proces.* 2014;2:419-440
44. Quigley MN. Student preparation of standard solutions. *J. Chem. Edu.* 2011;68(6):505-509
45. Nguyen VT, Tran TH. Application of chitosan solutions for rice production in Vietnam. *Afr. J. Biotech.* 2013;12(4):382-384
46. Altaher H. Preliminary study of the effect of using biosorbents on the pollution of the treated water. *Glob. NEST Jour.* 2014;16(10):1-10
47. Sen TK. Review on Dye Removal from Its Aqueous Solution into Alternative Cost Effective and Non-Conventional Adsorbents. *J Chem. Proc. Eng.* 2014;1:1-11
48. Zeroual Y, Kim BS, Kim CS, Blaghen M, Lee KM. Biosorption of Bromophenol Blue from Aqueous Solutions by *Rhizopus Stolonifer* Biomass. *Wat., Air, and Soil Poll.* 2016;1(4):135-146
49. Hasan S, Fuat G, Gülbahar AS. Using grape pulp as a new alternative biosorbent for removal of a model basic dye. *Asia-Pac. J. of Chem. Eng.* 2014;9(2):1-10
50. Alabi O, Alade AO, Afolabi TJ. Process optimization of adsorption of Cr(VI) on adsorbent prepared from *Bauhinia rufescens* pod by Box-Behnken Design, *Sep. Sci. Technol.* 2019;
51. Thitame PV, Shukla SR. Adsorptive removal of reactive dyes from aqueous solution using activated carbon synthesized from waste biomass materials. *Int. J. Environ. Sci. Technol.* 2016;13:561–570
52. Inyinbor AA, Adekola FA, Olatunji GA. Adsorption of Rhodamine B Dye from Aqueous Solution on *Irvingia gabonensis* Biomass: Kinetics and Thermodynamics Studies. *South. Afr. J. Chem.* 2015;68:115-125
53. Feng-Chin W, Ru-Ling T, Ruey-Shin J. Characteristics of Elovich Equation Used for The Analysis of Adsorption Kinetics in Dye-Chitosan Systems. *Che. Eng. J.* 2009; 150(2-3): 366-373
54. Idris S, Iyaka YA, Ndamitso MM, Mohammed EB, Umar MT. Evaluation of Kinetic Models of Copper and Lead Uptake from Dye Wastewater by Activated Pride of Barbados Shell. *Am. J. Chem.* 2011;1(2):47-51
55. Hesas RH, Wan Daud WA, Sahu JN, Arami NA. Preparation and Characterization of Activated Carbon from Apple Waste by Microwave Assisted Phosphoric Acid Activation. *Bio Resourc.* 2013; 8(2):2950-2966
56. Ponnusami V, Sunil K, Gunasekar V. Removal of Methylene Blue from Aqueous Effluent Using Fixed Bed of Groundnut Shell Powder. *J. Chem.* 2013;1-5
57. Yusoff MS, Mohammadizaroun M. Review on Landfill Leachate and Wastewater Treatment Using Physical-Chemical Techniques: Their Performance and Limitations. *Int. J. Curr. Lif. Sci.* 2014;4(12):12068-12074
58. Senthilkumaar S, Krishna SK, Kalaamani P, Subburamaan CV, Ganapathi S. Adsorption of Organophosphorous Pesticide from Aqueous Solution Using Waste Jute Fiber Carbon. *Mod. Appl. Sci.* 2010;4(6):422-434
59. Murali K, Uma RN. Removal of Basic Dye (Methylene Blue) Using Low Cost Biosorbent: Water Hyacinth. *Int. J. Adv. Eng. Technol.* 2012;1-15
60. Bello OS, Auta M, Ayodele OB. Ackee Apple (*Blighia sapida*) seeds: a novel adsorbent for the removal of Congo Red dye from aqueous solutions. *Chem. Ecol.* 2012;29(1):23-35
61. Asma N, Hizbullah K, Amir S, Zakaria M, Nawshad M, Muhammad IK. Potential Biosorbent Derived from *Calligonum polygonoides* for Removal of Methylene Blue Dye from Aqueous Solution. *Sci. Worl. Jour.* 2015; 1:1-11
62. Jeyabalan T, Praveen P. Degradation of Dyes (Methylene Blue and Congo Red Dye) Using Phosphomolybdic Acid. *Int J. Sci. Res.* 2012;3:2319-7064
63. Nimkar DA, Chavan SK. Removal of Congo red Dye from Aqueous Solution by Using Saw Dust as an Adsorbent. *Int. J. of Eng. Res. Applic.* 2014;4(4):47-51
64. Khalifa R, Safa C, Béchir BT. Adsorption of Methylene Blue Dye onto Aleppo Pine (*Pinus Halepensis* Mill.) Fibers: A Kinetic Modeling Studies. *Elix. Chem.Eng.* 2016;97:42317-42322
65. Salman JM, Amrin AR, Hassan MH, Jouda SA. Removal of congo red dye from aqueous solution by using natural materials. *Mesop. Env. Jour.* 2015;1(3):82-89
66. Asfaram A, Fathi MR, Saeid K, Naraki M. Removal of Direct Red 12B by garlic peel as a cheap adsorbent: Kinetics, thermodynamic and equilibrium isotherms study of removal. *Spectr. Acta Part A Molec. Biomolec. Spectr.* 2014;127(2):415-421
67. Wanyonyi WC, Onyari JM, Shiundu P. Adsorption of Congo Red Dye from Aqueous Solutions Using Roots of *Eichhornia Crassipes*: Kinetic and Equilibrium Studies. *Energy Procedia.* 2014;50:862–869

68. Ali A, Kovo A, Adetunji S. Methylene Blue, and Brilliant Green Dyes Removal from Aqueous Solution Using Agricultural Wastes Activated Carbon. *J. of Encapsul. Adsorp. Sci.* 2017;7: 95-107
69. Kim D.-S, Se-Jin O, Ijagbemi CO, Baek M-H. Removal of Malachite Green from aqueous solution using degreased coffee bean. *J. Hazard. Mater.* 2010;176(1-3):820–828
70. Adebayo GB, Adegoke HI, Jamiu W, Balogun BB, Jimoh AA. Adsorption of Mn(II) and Co(II) ions from aqueous solution using Maize cob activated carbon: Kinetics and Thermodynamics Studies. *J. Appl. Sci. Env. Man.* 2015;19(4):737-748
71. Ramachandra TV, Ahalya N, Kanamadi RD. Biosorption: Techniques and Mechanisms. *CES Tech. Rep.* 2013;110
72. Mohammad SA, Rexona K, Mohammad AR. Removal of Congo Red Dye from Industrial Wastewater by Untreated Sawdust. *Am. J. Environ. Protect.* 2015; 4(5):207-213
73. Hameed BH. Evaluation of papaya seeds as a novel non-conventional low-cost adsorbent for removal of methylene blue. *J. Hazard. Matter.* 2009;162 (2-3):939-944
74. Hu Z, Chen H, Ji F, Yuan S. Removal of Congo Red from aqueous solution by cattail root. *J. Haz. Mat.* 2010; 1(3):292-297